

24. NORMAL DUCTILE SHEAR ZONES AT AN OCEANIC SPREADING RIDGE: TECTONIC EVOLUTION OF SITE 735 GABBROS (SOUTHWEST INDIAN OCEAN)¹

Mathilde Cannat,² Catherine Mével,³ and Debra Stakes⁴

ABSTRACT

We detail the downhole evolution of the ductile deformation in the Site 735 gabbros, using deformed textures as indicators of relative finite-strain intensities, synkinematic metamorphic assemblages as indicators of temperature ranges and of availability of hydrothermal water during deformation, and the size of dynamically recrystallized plagioclase grains as an indicator of relative deviatoric stress intensities. Based on these data, and on the geometry and kinematics of the ductile shear bands throughout the hole, we propose that the ductile deformation recorded at Site 735 resulted from tectonic stretching of the newly accreted gabbroic material at and near the axis of the Southwest Indian Ridge. Apparent changes in the rheological behavior of the gabbros during this extensional ductile deformation suggest a three-step tectonic evolution at progressively lower temperatures and increased availability of hydrothermal water.

INTRODUCTION

Peridotites and gabbros constitute about 50 wt% of the rocks dredged along the Southwest Indian Ridge and transform plate boundary (Fisher et al., 1986), where the spreading rate is low (0.8–1 cm/yr; Fisher and Sclater, 1983). Most of these deep-seated rocks come from scarps on transform faults, but 12% of the ultramafics and 2% of the gabbros come from rift valley walls (Fisher et al., 1986). Along scarps of the Atlantis II Fracture Zone itself, dredges (Fisher et al., 1986; Dick et al., this volume) also recovered a significant proportion of peridotites (about 30%) and of gabbros (16%). Recent models to explain this emplacement of deep crustal rocks and of upper mantle material in the seafloor involve large-scale normal faulting of the newly created oceanic lithosphere (Dick et al., 1981; Karson and Dick, 1984; Karson, in press). Earlier models explained the exposure of ultramafic rocks in the seafloor by serpentinite diapirism, following the penetration of seawater along faults into the upper mantle (Bonatti and Honnorez, 1976; Francis, 1981). The tectonic exposure of gabbroic and ultramafic rocks may also be facilitated in accretionary environments where the crust is thin because of low magmatic budgets (CAYTROUGH, 1979; Fox et al., 1980; Cannat et al., 1990; Mével et al., in press).

Gabbros drilled at Site 735 during Ocean Drilling Program (ODP) Leg 118 crop out on a shallow platform (700 m water-depth), on the eastern wall of the Atlantis II Fracture Zone (Southwest Indian Ocean; Fig. 1). The 435 m of almost continuous core recovered at this drill site is a unique material for studying the magmatic and tectonic processes active in a portion of deep oceanic crust that ultimately will be uplifted and emplaced in the seafloor. This study concerns the tectonic evolution of the Site 735 gabbros. We show the existence of low-angle, ductile, normal shear zones that were active at high temperatures, probably when the gabbros were still in deep

levels of the rift valley domain. Movements along these normal shear zones probably led to thinning of the young oceanic lithosphere and to substantial uplift of the gabbro section.

Gabbros plastically deformed at high temperatures have been collected at a number of locations along slow-spreading ridges and fracture zones (Bonatti et al., 1975; Helmstaedt and Allen, 1977; CAYTROUGH, 1979; Ito and Anderson, 1983; Honnorez et al., 1984; Karson and Dick, 1984; Stakes and Vanko, 1986; Mével, 1987, 1988). But the gabbro section drilled at Site 735 provides an opportunity to determine the geometry and kinematics of such high-temperature deformation and its relationships with mid-ocean ridge magmatic and hydrothermal processes, which is the purpose of this study. The relative timing and geometry between the ductile and brittle deformations in the gabbros are also described. We integrate the results presented in two companion papers: one on the mechanisms of ductile deformation (Cannat, this volume), and the other on metamorphic petrology (Stakes et al., this volume) of the Site 735 gabbros. These results are compiled from shipboard visual core and thin section descriptions, from a detailed survey of the macroscopic deformational structures in the cores, and from microstructural and mineralogical study of a set of 200 additional samples distributed throughout the hole. Many of these samples are "oriented," meaning that the original attitude of the vertical has been preserved. The dips of the structures, and the kinematics of the vertical component of the deformation, therefore can be defined. In addition, we use the indications given by Cannat and Pariso (this volume) about the direction of dip of the deformational structures relative to one another and to the remanent magnetic vector at Site 735. These indications are based on the assumption, supported by paleomagnetic measurements (Shipboard Scientific Party, 1989; Pariso et al., this volume), that the remanent magnetic vector in each piece of core pointed in the same direction before drilling.

TECTONIC SETTING AND LITHOSTRATIGRAPHY AT SITE 735

Site 735 is located about 90 km south of the Southwest Indian Ridge axis, at the crest of the eastern wall of the Atlantis II Fracture Zone (Fig. 1). The age of the crust at Site 735, calculated by knowing the distance to the ridge axis and

¹ Von Herzen, R. P., Robinson, P. T., et al., 1991. *Proc. ODP, Sci. Results*, 118: College Station, TX (Ocean Drilling Program).

² GDR "Génèse et Evolution des domaines Océaniques," UBO, 6 Av. Le Gorgeu, 29287 Brest Cedex, France.

³ Laboratoire de Pétrologie, Université de Paris VI, 4 Pl. Jussieu, 75251 Paris Cedex 05, France.

⁴ Department of Geological Sciences, University of South Carolina, Columbia, SC 29208, U.S.A.

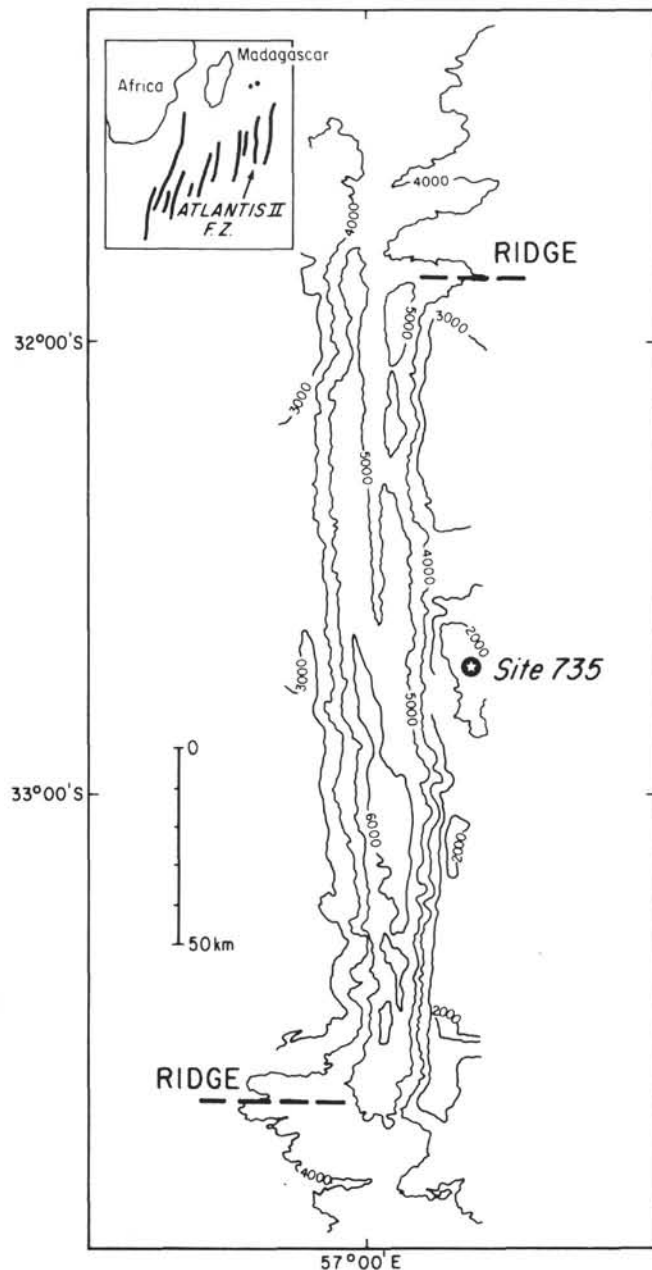


Figure 1. Bathymetric map of the Atlantis II transform fault, showing the location of Site 735. Contour intervals at 1000 m. Survey from *Conrad* cruise 27-09, 1986; H. Dick, Chief Scientist, with D. Gallo and R. Tyce.

the spreading rate, is about 11 Ma. This estimate agrees with the interpretation of the magnetic anomaly pattern over the area (Dick et al., this volume) and with the radiometric ages of magmatic zircon from the Site 735 gabbro section (J. Mattinson, pers. comm., 1989). Site 735 lies about 18 km east of the inferred active axis of the transform fault (Fig. 1). The crust at Site 735 thus was probably accreted about 11 m.y. ago, about 18 km from the ridge/transform intersection.

Site 735 lies on a shallow platform in about 700 m of water. This platform, 9 km long and 4 km wide, is one of a series of similar elevated blocks that form a transverse ridge along the eastern wall of the Atlantis II Fracture Zone (Fig. 1). The elevation of these blocks is greater than that predicted by the thermal subsidence of newly created oceanic lithosphere, and a gravity survey indicates that these elevated blocks are

underlain by high density material (Snow et al., unpubl. data), in agreement with the presence of gabbros at the outcrop at Site 735.

The Leg 118 shipboard scientists identified six lithologic units at Site 735 (Shipboard Scientific Party, 1989; Fig. 2). Unit I (Cores 118-735B-1D-1 to 118-735B-10D-1; 0 to 37.5 m below seafloor [mbsf]) comprises an upper subunit of foliated metagabbro (down to Core 118-735B-7D-1) and a lower subunit of mixed gabbro and olivine gabbro. Unit II (Cores 118-735B-10D-2 to 118-735B-35R-6; 37.5 to 170.2 mbsf) is made of olivine gabbro with intervals of oxide gabbro. Unit III (Cores 118-735B-35R-6 to 118-735B-46R-3; 170.2 to 223.6 mbsf) comprises mixed disseminated oxide olivine gabbro and olivine gabbro with intervals of oxide gabbro. Unit IV (Cores 118-735B-46R-3 to 118-735B-56R-4; 223.6 to 275 mbsf) is composed of oxide gabbro. Unit V (Cores 118-735B-57R-1 to 118-735B-73R-7; 275 to 374.5 mbsf) is composed of olivine gabbro. Unit VI (Cores 118-735B-73R-7 to 118-735B-88N; 374.5 to 500.7 mbsf) comprises olivine-rich gabbro with intervals of oxide gabbro and troctolite. Lastly, Site 735 gabbros are locally intruded by small volumes of evolved leucocratic melts, which are particularly abundant in the gabbros of Units IV and V (Fig. 2). The recovery rates were: 36.5% in Unit I; 80.3% in Unit II; 104.6% in Unit III; 108% in Unit IV; 98% in Unit V; and 103% in Unit VI (rates greater than 100% indicate that material left over from the overlying cores was recovered). The low recovery in Unit I probably resulted from the use of a motor-driven bit. Recovery was greatly improved below Core 118-735B-11D by the use of rotary-driven bits. These high recovery rates allow us to assume that, except in the uppermost part of the hole, most of the deformed gabbros at Site 735 were recovered.

The lithostratigraphic column in Figure 2 also indicates the location of the 1- to several meter-thick mylonitic intervals occurring throughout the hole. The 5-m-thick mylonitic band at Cores 118-735B-5D and 118-735B-6D (21–26 mbsf) occurs within Unit I. It coincides with the contact set by shipboard scientists between the upper metagabbro subunit and the underlying mixed gabbro and olivine gabbro subunit. The mylonitic band at Cores 118-735B-9D and 118-735B-10D (35.7–36.5 mbsf) is located 1 m above the Unit I/Unit II contact (Fig. 2). The meter-thick mylonitic band at Core 118-735B-46R (223–224 mbsf; Figs. 2 and 3) coincides with the limit set by shipboard scientists between Units III and IV (mixed disseminated oxide olivine gabbro and olivine gabbro with intervals of oxide gabbro) and IV (oxide gabbro). However, there is no clear-cut lithological contrast across this mylonitic shear zone: olivine gabbros with intervals of Fe-Ti oxide gabbros are found above and below. Furthermore, the gabbros of Units III and IV have a well-developed planar fabric, thought to be mostly magmatic in origin (see below); this planar fabric is cut by the shear zone and has the same dip above and below it (Fig. 3). We propose that the transition between Units III and IV, marked by an increase in the frequency and thickness of oxide-rich intervals, is magmatic, not tectonic, in origin. The 2-m-thick mylonitic shear zone at Core 118-735B-56R (270–272 mbsf) was initially interpreted by shipboard scientists as a tectonic contact between the oxide gabbro of Unit IV and the olivine gabbro of Unit V. This interpretation has been revised, as subsequent sampling showed that undeformed to moderately deformed oxide gabbros occur below this shear zone. The mylonitic shear zone of Core 118-735B-56R thus is interpreted as an intra-unit shear zone. The contacts between Units II and III, and between Units V and VI, do not coincide with deformed intervals (Fig. 2).

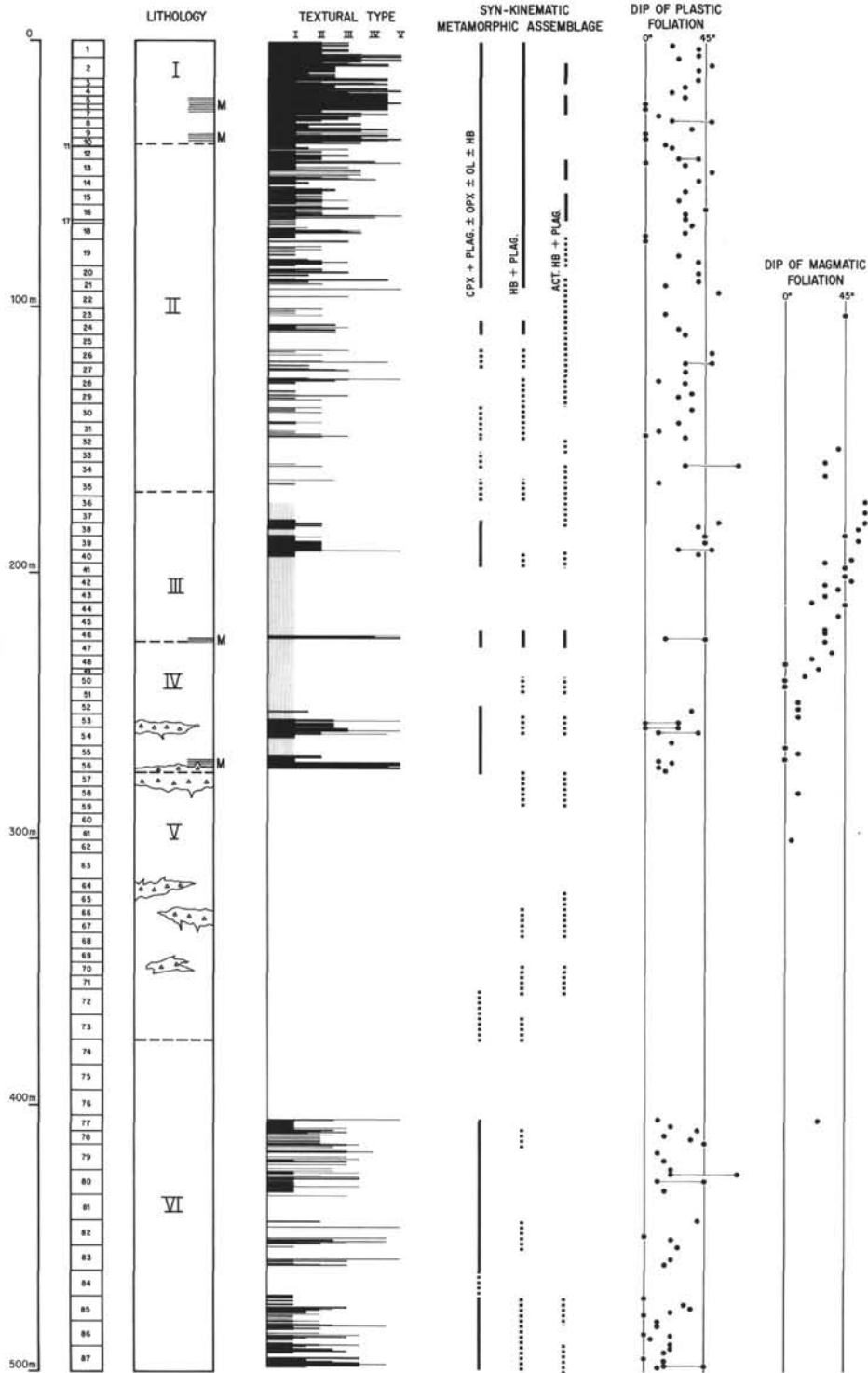


Figure 2. Lithological and structural stratigraphy at Site 735. From left to right: depth below seafloor; core numbers; lithostratigraphy (see text), M. = mylonitic shear zone, small triangles: late magmatic liquids; textural types (see Fig. 5), the interval having well-developed magmatic foliations is shaded; synkinematic assemblages (see text), CPX = clinopyroxene, PL = plagioclase, OL = olivine, OPX = orthopyroxene, HB = hornblende, and ACT HB = actinolitic hornblende; the dashed lines cover intervals where synkinematic crystallization of a given assemblage is limited, either because deformation is weak, or because it occurred mostly under the stability conditions of another assemblage (see text); dip of solid-state plastic foliation (dotted lines join the dip of the main foliation with that of steeper secondary shear bands); dip of magmatic foliation (see text).

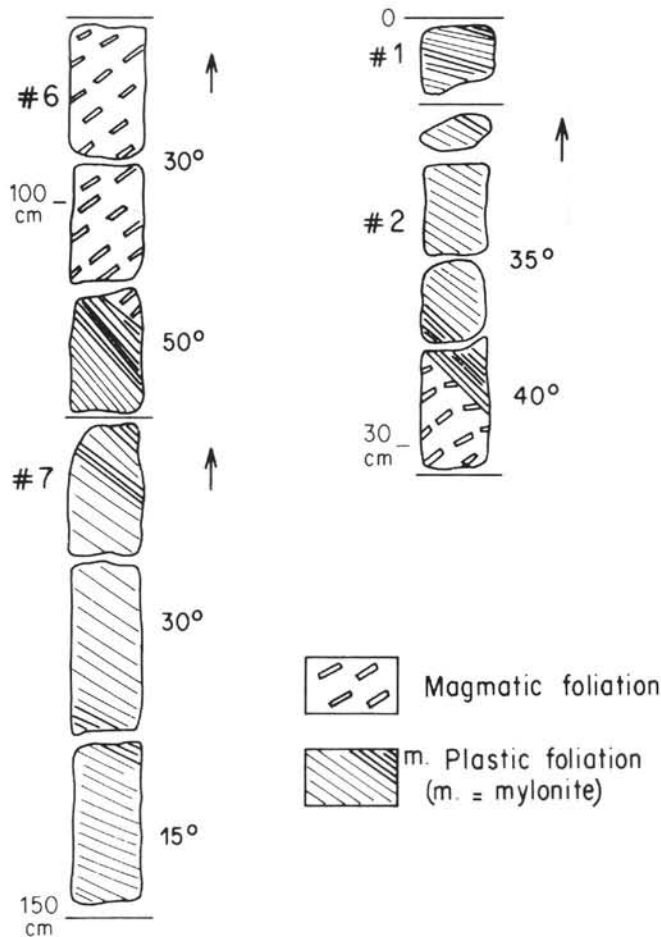


Figure 3. Mylonitic shear zone at Core 118-735B-46R (223–224 mbsf); see text for definition of magmatic and plastic foliations.

DUCTILE FLOW IN THE SITE 735 GABBROS

Magmatic Flow

Some Site 735 gabbros display a foliation marked by the planar disposition of anhedral to euhedral plagioclase crystals, and/or of subeuhedral to anhedral clinopyroxene and olivine grains (Fig. 4A). This foliation often parallels a centimeter-scale compositional layering and is best expressed in the hole between 170 and 270 mbsf (Fig. 2), in the oxide-bearing gabbros of Units III and IV. In thin sections, one clearly sees that this foliation was not produced by significant intracrystalline deformation: the minerals are seldom recrystallized, and subgrain boundaries and mechanical twins are scarce. However, the crystallographic-preferred orientation of plagioclase is strong (Cannat, this volume) and recalls that of other gabbros thought to have been deformed in the magmatic state (Benn and Allard, 1989). The development of this foliation is attributed to laminar viscous flow of the incompletely crystallized magma (Cannat, this volume). The limited dynamic recrystallization and the mechanical twins observed in the plagioclase of these magmatically foliated gabbros, and the sporadic subgrain boundaries in olivine, reflect a weak overprint of solid-state deformation. This limited solid-state deformation is thought to result from the last stages of flow within the progressively solidifying gabbros.

The magmatic foliation (Fig. 4A), with its weak overprint of solid-state deformation, dips 55° to 60° (estimated degree of error: +10°) in Cores 118-735B-35R to 118-735B-38R (170–180

mbsf; Fig. 2). A weak downdip lineation is locally marked by the preferred orientation of the long axis of the plagioclase, clinopyroxene, and olivine crystals. The dip of the magmatic foliation decreases progressively downward, from 0° to 10° in Core 118-735B-50R (238 mbsf; Fig. 2). The partial reorientation data presented by Cannat and Pariso (this volume) suggest that all magmatic foliations at Site 735 dip approximately in the same direction, with a dominant dip azimuth at a 320° angle, clockwise, from the direction of the *in-situ* paleomagnetic vector. The progressive downward decrease of the dip of these magmatic foliations is not accompanied by an increase, or a decrease, of the solid-state deformation. It is also not accommodated by discrete solid-state shear zones. As a matter of fact, the interval located between Cores 118-735B-41R and 118-735B-50R, where most of the rotation occurred (Fig. 2), is almost free of solid-state deformation bands. The only highly deformed shear zone in this interval is the mylonitic band at Core 118-735B-46R, which crosscuts the magmatic foliation at a wide angle (Fig. 3). We therefore propose that the downward rotation of the magmatic foliation in Units III and IV was achieved before the gabbro was completely solidified.

Solid-State Ductile Deformation

Finite Strain, Foliation, Lineation, and Sense of Shear Determinations

The shipboard description of the plastically deformed gabbros (Shipboard Scientific Party, 1989) was based on the distinction of five textural types (Fig. 5). Type I is weakly deformed, with no penetrative foliation and little recrystallization of plagioclase. In Type II textures, the elongation of the constituting minerals defines a pervasive foliation, but the dynamic recrystallization of plagioclase is still limited. Type III is well foliated, with extensive dynamic recrystallization of plagioclase and a significant reduction of the mean size of the clinopyroxene, orthopyroxene, oxide, and olivine porphyroclasts. In Type IV, the plagioclase is also extensively recrystallized, and millimeter-thick mylonitic bands are present (Fig. 6). Type V is mylonitic. The term "mylonitic" is used here for high-strain intervals with reduced grain size. The downhole distribution of these five textural types, based on the macroscopic description of the cores and confirmed under the microscope for each available thin section, is shown in Figure 2.

We did not find reliable indicators for finite strain intensity measurements in the Site 735 gabbros. The elongation of the recrystallized tails of mafic minerals in Types III to V (Figs. 5C and 5D) certainly suggests large strain, but the original size of the deformed crystals is difficult to assess. In the mylonites, the number of rotations achieved by the rounded porphyroclasts (Fig. 5D) in the foliation is also impossible to know. It is, however, possible to estimate the relative finite strain intensities, using the textural types defined in the above paragraph. Most Site 735 gabbros contain more than 50% plagioclase. The plastic deformation of this mineral appears to have been controlled by dislocation slip and by dynamic recrystallization (Cannat, this volume). The transition from Type I to Type III textures, marked by the increasing dynamic recrystallization of plagioclase (Fig. 5), thus probably corresponds with an increase of the finite strain. The development of mylonites in Types IV and V indicates a further increase of the strain. The textural types column in Figure 2 thus may be read as an indicator of relative (solid-state) finite strain intensities throughout the hole. The strain gradients in the plastically deformed gabbros of Site 735 are often steep, and textures corresponding to highly contrasting strain intensities

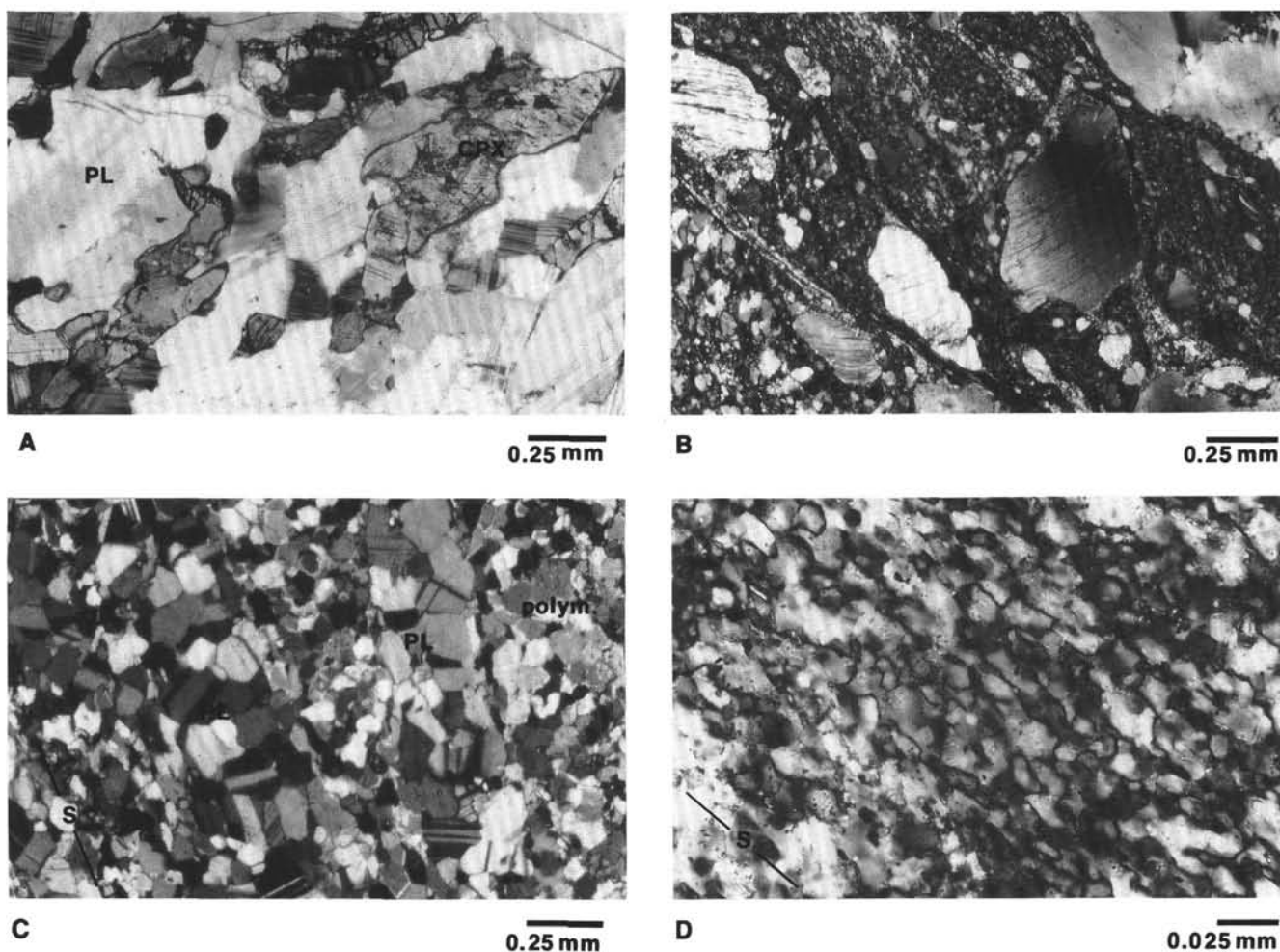


Figure 4. Photomicrographs from Site 735. Crossed nicols. PL = plagioclase; OL = olivine; CPX = clinopyroxene; Hb = hornblende; Act. Hb = actinolitic hornblende; S = trace of foliation; L = stretching lineation. **A.** Magmatic foliation defined by tablet-shaped olivine and clinopyroxene crystals in anhedral plagioclase; Sample 118-735B-38R-4, 10–15 cm. **B.** Shear band with finely recrystallized plagioclase and hornblende, Sample 118-735B-31R-3, 53–61 cm; the asymmetric tails around clinopyroxene porphyroclasts indicate a sinistral sense of shear, corresponding to a normal displacement in the core. **C.** Polygonal plagioclase neoblasts in Sample 118-735B-80R-1, 11–17 cm; the trace of the foliation is defined by elongate streaks of recrystallized plagioclase, alternating with finer grained polymineral (olivine, plagioclase, clinopyroxene and hornblende) recrystallized aggregates (Polym.). **D.** Fine-grained recrystallized plagioclase in Sample 118-735B-1D-2, 85–89 cm; the recrystallized grains have irregular grain boundaries, they are slightly elongated in the foliation; there are no mechanical twins, but undulatory extinctions are frequent. **E.** Aggregate of relatively large polygonal plagioclase neoblasts cut by a latter microshear (S2), with small and irregularly shaped recrystallized plagioclase; Sample 118-735B-87R-5, 44–47 cm; note the wavy extinction in the large plagioclase neoblasts near the microshear. **F.** Limited recrystallization of plagioclase in small, irregularly shaped neoblasts in late magmatic leucocratic injection from Sample 118-735B-53R-4, 5–15 cm. **G.** Cataclastic breccia with fractures filled with undeformed crystals of actinolitic hornblende; Sample 118-735B-52R-2, 83–89 cm. **H.** Kinked and fractured plagioclase porphyroclast in Sample 118-735B-8D-1, 17–20 cm; the cracks are subperpendicular to the stretching lineation of the sample, and filled with green to brown hornblende.

are commonly juxtaposed. In practice, such small-scale heterogeneities cannot be represented in the textural log. Our work is based on a textural log drawn at a scale of 1:100 (Fig. 7). This means that the textural heterogeneities occurring in intervals less than about 10 cm thick are empirically averaged in the textural log. For example, the 10-cm-thick interval of Figure 6 is plotted in the log between textural Types IV and V. As a consequence, the frequency of the mylonitic intervals, which are often less than 10 cm thick, is underestimated in the textural log of Figure 2.

The dip of the solid-state plastic foliations at Site 735, measured with a degree of error estimated at $\pm 10^\circ$, is 45° , or less, in most deformed intervals (Fig. 2). As for textural types, the foliation dip data presented in Figure 2 are simplified from our working log, drawn at a scale 1:100 (Fig. 7) and showing the foliation dip in each deformed oriented core piece through-

out the hole. The partial reorientation data presented by Cannat and Pariso (this volume) suggest that most solid-state foliations at Site 735 dip in approximately the same direction, at 260° to 330° , clockwise, from the direction of the *in-situ* paleomagnetic vector. All foliated gabbro samples also exhibit a lineation, marked by elongated minerals, or by streaks of recrystallized grains. This stretching and mineral lineation is near downdip in most samples, indicating that the solid-state plastic deformation at Site 735 resulted from dominantly vertical displacements. The sense of shear indicators in the deformed gabbros are (1) asymmetric pressure-shadows and tails of recrystallized grains around rotated porphyroclasts (Fig. 4B), (2) the obliquity between mylonitic shear bands and the foliation in the less-deformed surrounding gabbros (Figs. 8 and 9), (3) drag-folds of an earlier foliation along later shear zones (Fig. 9), and (4) the asymmetry of olivine preferred

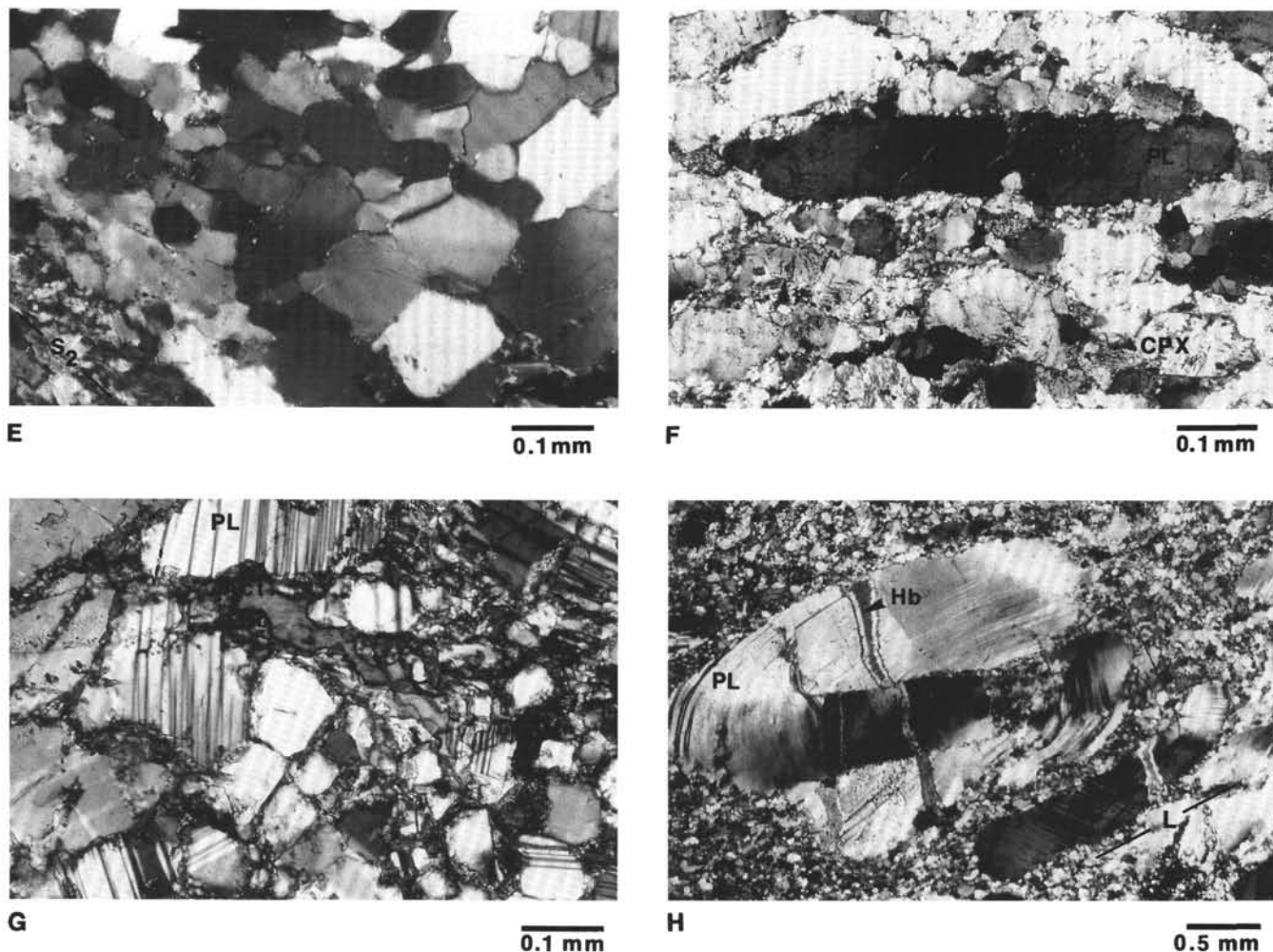


Figure 4 (continued).

orientation fabric diagrams relative to the samples foliation and lineation (Cannat, this volume). The "sense of shear" column in Figure 10 shows that the vertical displacement during solid-state plastic deformation at Site 735 was predominantly normal.

Synkinematic Metamorphic Conditions

The mineralogy and mineral chemistry of the metamorphic assemblages in the Site 735 gabbros are described in a companion paper (Stakes et al., this volume). The main conclusion of this detailed study is that the plastic deformation at Site 735 occurred in high-temperature conditions, which suggests that it occurred near the ridge axis. Minerals are described as part of a synkinematic metamorphic assemblage if they crystallized, or recrystallized together, in the plastic foliation. The petrographic criteria used to determine if distinct minerals crystallized or recrystallized together are the presence of clean grain boundaries and of frequent triple junctions. Such textures do not necessarily mean, however, that metamorphic equilibrium was achieved: synkinematic amphibole, for example, often exhibits compositional zoning, suggesting a progressive lowering of the temperature (Stakes et al., this volume). For this reason, each metamorphic assemblage is interpreted as characteristic of a range of metamorphic conditions. Three broad types of synkinematic

assemblages are distinguished in Figure 2. The first assemblage is similar in mineralogy and in mineral compositions (Stakes et al., this volume) to the magmatic primary assemblage: calcic plagioclase + clinopyroxene \pm olivine \pm orthopyroxene \pm Fe-Ti oxide \pm brown to green hornblende. This first assemblage covers the temperature range between the granulite facies (recrystallized orthopyroxene), and the upper amphibolite facies (no recrystallization of orthopyroxene). Of course, it is possible to distinguish between these two facies in deformed orthopyroxene-bearing gabbros, and recrystallized orthopyroxene was observed, at least in one sample, in many high-temperature shear zones throughout the hole.

However, we found it impossible to distinguish reliably between these two facies in the synthetic log of Figure 2, because many intervals at Site 735 do not include primary orthopyroxene. The second assemblage is characterized by an abundance of euhedral brown to green hornblende. The primary mafic minerals did not recrystallize, but the dynamically recrystallized plagioclase was still compositionally similar to the relict magmatic porphyroclasts (Stakes et al., this volume). The range of temperatures estimated for this second assemblage is near that estimated for the first assemblage, when no recrystallization of orthopyroxene occurred, but the water-rock ratio was higher. The third synkinematic assemblage is present only in a few samples; it consists of less calcic

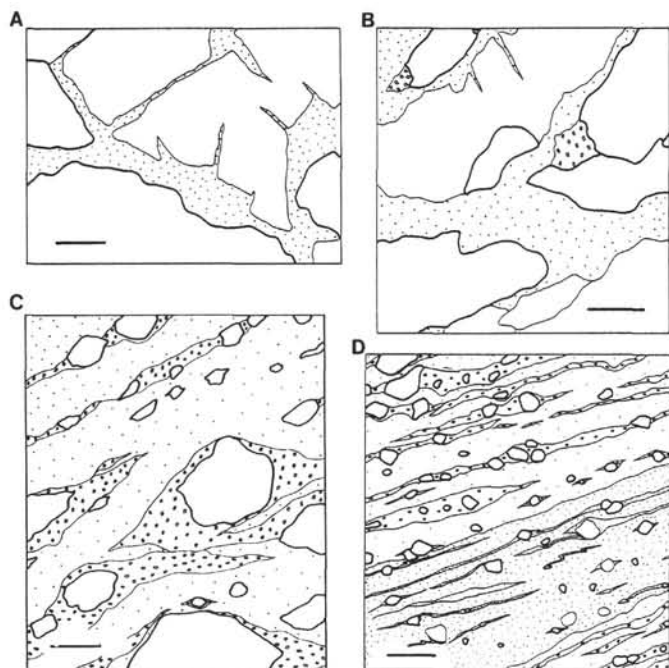


Figure 5. Sketches of deformed textures in Site 735 gabbros. Scale bar is 1 mm. Heavy contours: mafic porphyroclasts, mostly clinopyroxene; light contours: plagioclase porphyroclasts; dots: recrystallized plagioclase; little squares: recrystallized mafic minerals. A. Sample 118-735B-2D-2, 0–4 cm; textural Type I: weakly recrystallized, unfoliated. B. Sample 118-735B-87R-2, 13–22 cm; textural Type II: moderately recrystallized, foliated. C. Sample 118-735B-2D-1, 56–62 cm; textural Type III: extensively recrystallized, well foliated. D. Sample 118-735B-3D-1, 46–49 cm; textural Type V: mylonitic; the closely spaced dots correspond to a band of finely recrystallized plagioclase and hornblende.

plagioclase + actinolitic hornblende. This third assemblage reflects slightly to distinctly lower temperatures than the second assemblage. Here, we refer to these three synkinematic metamorphic assemblages as assemblage¹ high-temperature (high T), low to moderate water/rock (W/R) ratio; assemblage² high T, high W/R ratio; and assemblage³ moderate T, high W/R ratio. A more detailed discussion of the synkinematic temperature ranges and W/R ratio conditions may be found in Stakes et al. (this volume).

The metamorphic data presented in Figure 2 is a simplified version of our working log (Fig. 7), which is based on the petrographic description of 185 plastically deformed samples distributed throughout the hole. The ductile deformation in a given interval often occurred over a range of decreasing temperature and increasing W/R ratio conditions. For example, the deformation in the upper part of the hole (Cores 118-735B-1D to 118-735B-21R; Figs. 2 and 7) began at high T and low W/R ratio (metamorphic assemblage¹), but continued at higher W/R ratio (metamorphic assemblage²) in most strongly deformed intervals. Lastly, the lower T, actinolitic hornblende-bearing assemblage³ developed in discrete shear zones. The dashed lines in Figure 2 cover the intervals where the synkinematic growth of a given metamorphic assemblage is limited, either because the total strain in this interval was small (as, for example, in Cores 118-735B-67R to 118-735B-73R; Fig. 2), or because most of the strain occurred under conditions of stability of another assemblage. For example, in the lower part of the hole (Cores 118-735B-53R to 118-735B-87R; Fig. 2), most deformation occurred under the stability conditions of metamorphic assemblage¹. Assemblage² and



Figure 6. A decimeter-thick mylonitic shear in textural Type IV gabbros. Sample 118-735B-2D-1, 134–149 cm. Ruler is vertical and points upward. Stretching lineation is down-dip. Roman numerals represent textural types (see text).

assemblage³ only developed locally, in discrete shear zones. The intrusions of evolved leucocratic melts crosscut most deformed intervals throughout the hole. However, they were locally sheared in the stability conditions of assemblage² and/or assemblage³.

Recrystallized Plagioclase Grain-Size as a Deviatoric Stress Indicator

Experimental evidence from metals, ceramics, and silicates (olivine, quartz, pyroxene), shows that during steady-state plastic flow, the grain size produced by dynamic recrystallization decreases as the applied deviatoric stress increases, regardless of the temperature or finite strain (Bird et al., 1969; Twiss, 1977; Mercier et al., 1977). There is no experimental evidence available for plagioclase. We propose, however, that the size of the dynamically recrystallized plagioclase in the Site 735 gabbros probably gives a relative estimate of the deviatoric stress during ductile deformation. A microstructural study (Cannat, this volume) suggests a sharp change of deformation processes in the Site 735 gabbros as temperature decreased from the stability conditions of granulite-facies metamorphic assemblages (assemblage¹ with recrystallized orthopyroxene) to the stability conditions of amphibolite-facies metamorphic assemblages (assemblage¹ with no recrystallized orthopyroxene, assemblage², and assemblage³).

Temperature-dependent diffusion processes appear to have controlled the deformation of all minerals in granulite-facies metamorphic conditions. In contrast, dislocation slip in plagioclase appears to have been the leading flow mechanism in gabbros deformed in amphibolite-facies metamorphic conditions (Cannat, this volume). This change in deformation processes correlates with a marked size decrease of the recrystallized

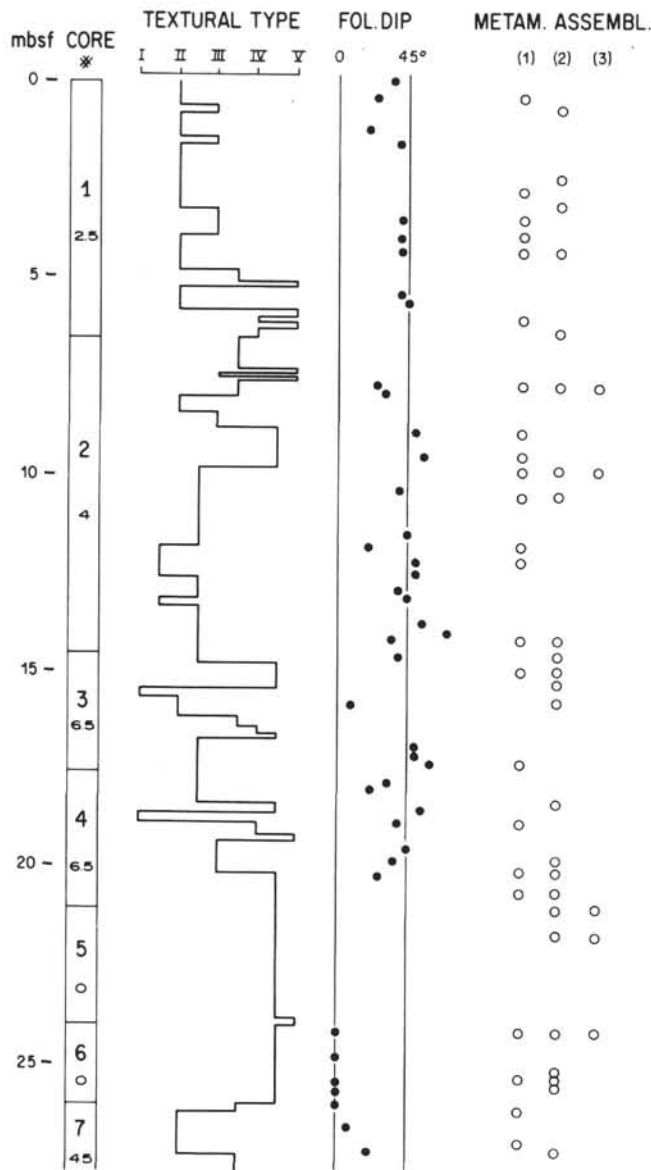


Figure 7. Our working log for textural types (see text), dip of solid-state plastic foliation, and synkinematic metamorphic assemblages (see text), between Cores 118-735B-1D-1 and 118-735B-7D-1. Figure 2 shows a simplified version of these data. The values in italic in each core represent the number of macroscopic veins per meter of core (see Stakes et al., this volume).

plagioclase grains, which is thought to result from an increase of the deviatoric stress, and thus from an increase of the yield strength of the gabbros. In gabbros deformed in granulite-facies metamorphic conditions, the recrystallized plagioclase grains are polygonal, with frequent triple junctions (Fig. 4C) and a bimodal size distribution: smaller neoblasts (10 to 40 μm) are surrounded by larger neoblasts (up to 2 mm in size) that are interpreted as resulting from grain-boundary migration (Cannat, this volume). Only the average size of the smaller neoblasts is given in Figure 10. In gabbros deformed in upper to lower amphibolite-facies metamorphic conditions, the recrystallized plagioclase grains are more irregular in shape, often with lobate grain boundaries (Fig. 4D). Their average size varies between 5 and 15 μm (Fig. 10).

The data presented in Figure 10 summarize recrystallized grain-size measurements in the 185 deformed samples also examined for synkinematic metamorphic assemblages. The

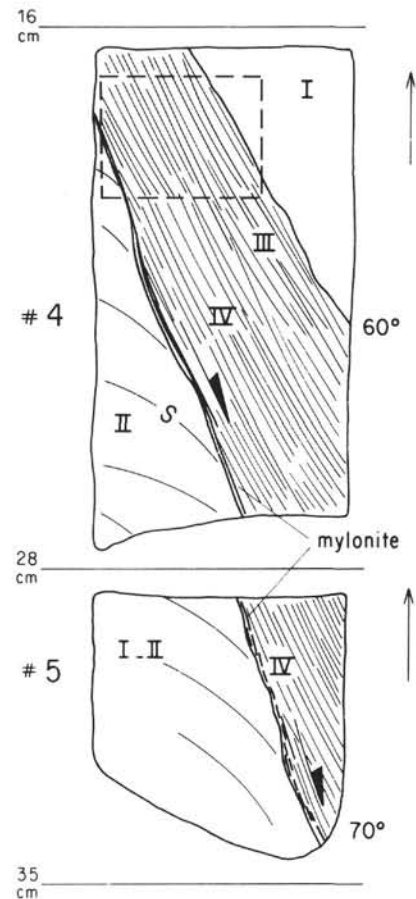


Figure 8. Sketch of steep normal shear band in Samples 118-735B-8D-1, 16-28 cm, and 118-735B-8D-1, 28-35 cm. Roman numbers represent textural types (see text); (S) = trace of foliation; dashed square = location of thin section photographed in Figure 4H.

average size of the recrystallized plagioclase in each thin section was visually estimated. Thus, the values presented in Figure 10 do not have the accuracy of statistical averages. Figure 10 shows that in many deformed intervals, the earlier, coarser-grained, recrystallized texture is overprinted by shearing in amphibolite-facies conditions, with development of small and irregularly shaped plagioclase neoblasts (Fig. 4E). In the intervals most strongly deformed in amphibolite-facies metamorphic conditions, such as the uppermost part of the hole (Cores 118-735B-1D to 118-735B-7D), or the narrow mylonitic shear zone at Core 118-735B-46R, intense dynamic recrystallization of plagioclase in fine-grained neoblasts left no relicts of the earlier, coarser-grained recrystallized texture. In the interval between Cores 118-735B-57R and 118-735B-71R, minor plastic deformation in amphibolite-facies metamorphic conditions (Fig. 2) produced fine-grained, irregular, plagioclase neoblasts (Fig. 10). Limited recrystallization of plagioclase in small and irregularly shaped neoblasts also affected some leucocratic melt intrusions.

Downhole Evolution of the Ductile Deformation

Based on the textural data summarized in Figure 2, we distinguished three structural domains at Site 735.

1. The Upper Structural Domain extends from Core 118-735B-1D to Core 118-735B-35R (0-172 mbsf). It is characterized by extensive development of the highly deformed Types III, IV, and V textures around the 5-m-thick mylonitic shear

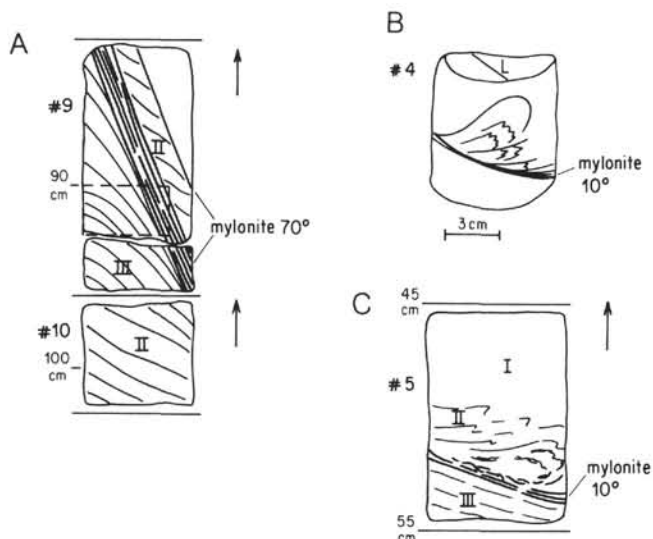


Figure 9. Normal microshears from the Lower Structural Domain. Roman numerals represent textural types (see text). **A.** Normal mylonitic shear band in Samples 118-735B-80R-1, 82-96 cm, and 118-735B-80R-1, 96-102 cm. **B.** **C.** Normal mylonitic shear zones accompanied by drag folds of an earlier foliation in Samples 118-735B-80R-1, 11-19 cm, and 118-735B-83R-5, 45-55 cm, respectively.

zone at Cores 118-735B-5D and 118-735B-6D (21-26 mbsf), and by the downward decrease of the finite strain below this shear zone.

2. The Middle Structural Domain extends between Core 118-735B-36R and the lower one-third of Core 118-735B-56R (172-272 mbsf). It is characterized by the development of a magmatic foliation, overprinted by solid-state ductile deformation in discrete intervals.

3. The Lower Structural Domain extends from the lower one-third of Core 118-735B-56R to the bottom of the hole (272-500.7 mbsf). The interval between the bottom of Core 118-735B-56R and Core 118-735B-76R (272-403 mbsf) is almost completely free of deformation. It is intruded by small volumes of late leucocratic melts. Below Core 118-735B-76R, the Lower Structural Domain gabbros are affected by discrete shear zones, with a limited development of the most deformed textural types.

Upper Structural Domain (Cores 118-735B-1D to 118-735B-35R; 0-172 mbsf)

The metagabbroites in Cores 118-735B-1D to 118-735B-5D are pervasively foliated and have textural Types II to V (Figs. 2 and 7). The foliation dips 10° to 50° , and the stretching lineation is dominantly downdip. The most deformed textures occur in decimeter-thick intervals (Fig. 6), in which the foliation is often steeper than in the less-deformed gabbros. This geometrical relation is consistent with a normal sense of shear. However, other sense of shear indicators, such as asymmetric pressure shadows or tails around rotated porphyroclasts, are scarce and often inconsistent in a given sample. Out of 15 oriented samples, only six yield a consistent sense of shear: normal in four cases, reverse in two (Fig. 10). The inconsistency of the sense of shear indicators suggests that deformation was heterogeneous (folds of the foliation with axis parallel to the stretching lineation). The synkinematic metamorphic assemblages usually include abundant recrystallized clinopyroxene (high T, low to moderate W/R ratio). But in most samples, the deformation is seen to continue, with the same geometry, under the higher W/R ratio conditions characterized by the

hornblende + plagioclase assemblage (Figs. 2 and 7). In a sample from Core 118-735B-2D (Fig. 7), actinolitic hornblende is also deformed and recrystallized in the foliation (medium T, high W/R ratio). The dynamically recrystallized plagioclase is irregularly shaped and small (about $10 \mu\text{m}$) in all samples (Figs. 4D and 10), suggesting that the deviatoric stress during the deformation was high.

The mylonitic foliation in the oriented pieces from Core 118-735B-6D is horizontal (Fig. 7). There are no oriented pieces in Core 118-735B-5D. The dominant synkinematic assemblage in the mylonites of Cores 118-735B-5D and 118-735B-6D is hornblende + plagioclase (high T, high W/R ratio). But recrystallized clinopyroxene is locally abundant, suggesting that the deformation began under lower W/R ratio conditions. In addition, in the samples from Core 118-735B-5D, the high T assemblages are deformed, with the same geometry, in the conditions of stability of actinolitic hornblende (Fig. 7). This suggests continuing deformation at decreasing temperature conditions. The sense of shear indicators are clear and consistent in any given sample, suggesting that the flow regime was rotational. The dynamically recrystallized plagioclase has the same irregular shape and small size (about $10 \mu\text{m}$) as in the overlying metagabbroites.

Below Core 118-735B-6D, the finite strain decreases markedly (Fig. 2). In Cores 118-735B-7D and 118-735B-8D, weakly deformed gabbros with no pervasive foliation alternate with well-foliated intervals. The foliation dips 10° to 30° , with scattered centimeter-thick mylonitic bands that dip 0° to 70° . The stretching lineation is dominantly downdip, and the sense of shear is normal (Fig. 8). The synkinematic assemblages include abundant recrystallized olivine and clinopyroxene, with scattered recrystallized orthopyroxene (high T, low W/R ratio). Synkinematic hornblende is locally abundant in Core 118-735B-7D (high T, high W/R ratio), but scarce in Core 118-735B-8D. In Cores 118-735B-9D and 118-735B-10D, the plastic deformation is intense again (textural Types III to V), with low-dipping foliations (0° to 20° ; Fig. 2). But, in contrast with the mylonitic shear zone of Cores 118-735B-5D and 118-735B-6D, this intense deformation occurred mostly in high T, low W/R ratio conditions, as shown by the scarcity of recrystallized hornblende in the foliation.

Below Core 118-735B-10D, deformation is moderate and its overall intensity decreases downward (Fig. 2). As in Cores 118-735B-7D and 118-735B-8D, intervals of undeformed, or weakly deformed gabbros are cut by centimeter- to meter-thick ductile shear bands, with Type II to V textures. The foliation in these shear bands dips 0° to 50° , and the stretching lineation is downdip. The sense of shear, determined in 14 samples, is dominantly normal (13 normal, one reverse; Fig. 10). The contacts between the shear bands and the surrounding undeformed gabbros are often sharp and frequently underlined by mylonites. The synkinematic metamorphic assemblages indicate high T, low to moderate W/R ratio conditions (Fig. 2). But the deformation continued locally, with the same kinematics, at lower T, in the conditions of stability of actinolitic hornblende.

Deformation of the gabbros in Cores 118-735B-7D to 118-735B-35R produced small (about $10 \mu\text{m}$), irregularly shaped plagioclase neoblasts (Fig. 10), similar to those observed in and above the mylonites of Cores 118-735B-5D and 118-735B-6D. But relicts of an earlier coarser-grained recrystallized texture are often found in the moderately deformed intervals.

The partial reorientation data presented by Cannat and Pariso (this volume) suggest that, in the Upper Structural Domain above and below the mylonitic shear zone of Cores 118-735B-5D and 118-735B-6D, the dip direction of the foliation is variable, but lies dominantly in the western sector, with

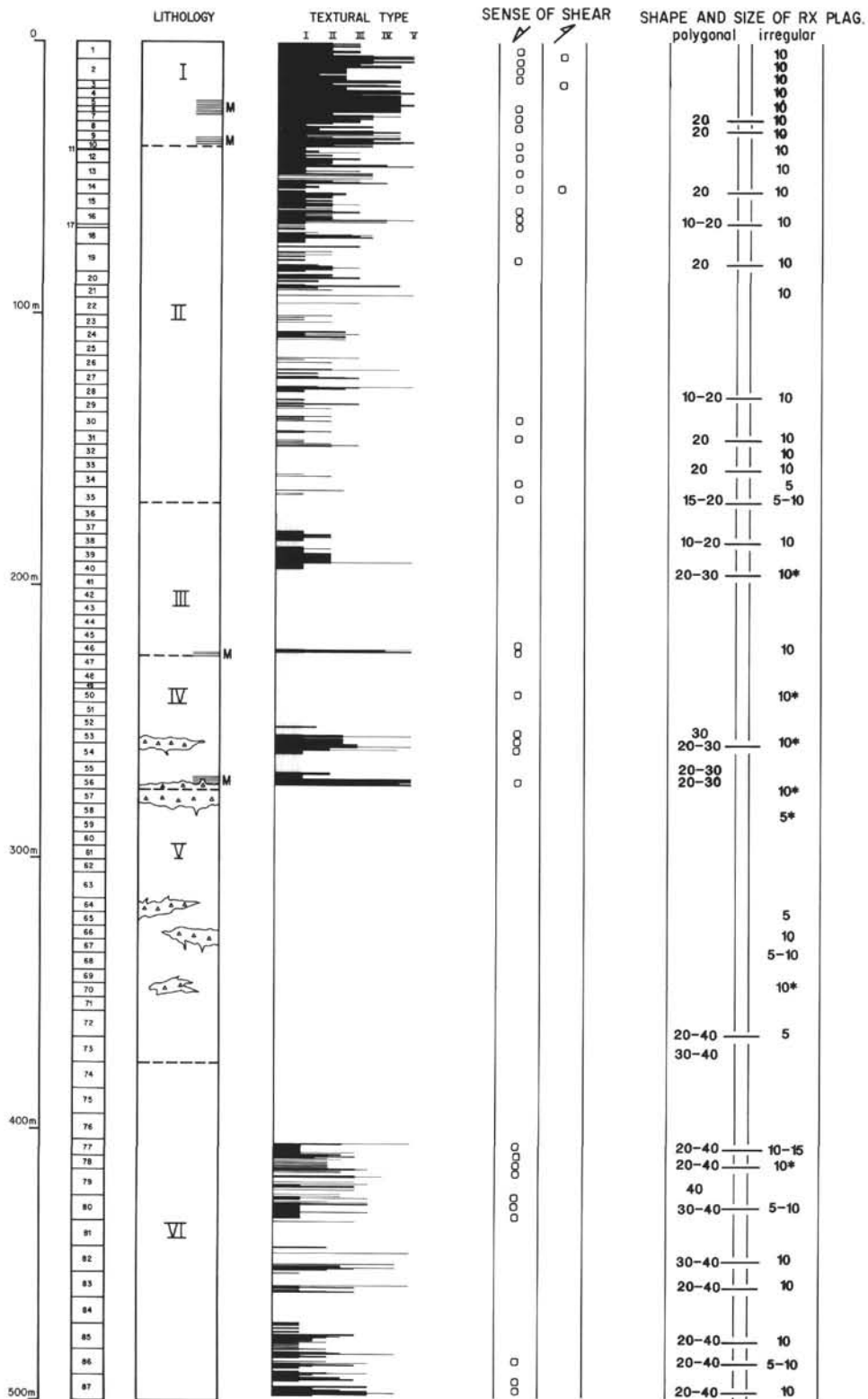


Figure 10. Lithological and structural stratigraphy at Site 735. From left to right: depth below seafloor; core numbers; lithostratigraphy (see text and caption Fig. 2); textural types (see text); sense of shear (normal or reverse; each dot corresponds to one sample); shape (polygonal or irregular) and approximate size (in μm) of the dynamically recrystallized plagioclase; lines join successive recrystallized grain sizes in samples showing two generations of dynamically recrystallized plagioclase; stars indicate that late magmatic leucocratic injections are also recrystallized.

respect to the remanent magnetic vector (V) taken as north. This is sketched in Figure 11A. The horizontal mylonites in Core 118-735B-6D make a significant angle with these foliations. One possible way to generate such contrasting foliation dips is sketched in Figure 11B: the foliation dip would progressively increase as finite strain decreased, away from a flat-lying shear zone. But the increase in dip of the foliation above and below Core 118-735B-6D does not appear to be progressive and does not correlate with decreasing finite strain (Fig. 7). The mylonites at Cores 118-735B-5D and 118-735B-6D more probably represent a flat-lying ductile fault, truncating steeper shear zones. The similarity of the microstructures and of the synkinematic metamorphic assemblages in, above, and below Core 118-735B-6D suggests that these steeper shear zones and the truncating flat-lying mylonites were active during a single deformation event. This would be the case if the mylonites of Cores 118-735B-5D and 118-735B-6D represented the flat-lying region of a listric ductile normal fault, and the steeper foliations a set of associated planar ductile faults. This is sketched in Figure 11C, which is an adaptation for ductile deformation of a model devised for brittle faults by Wernicke and Burchfield (1982). We are aware that this may not be the correct explanation: pieces of core 6 cm in diameter may only provide partial constraints on large-scale structures, and the mediocre recovery rates in Cores 118-735B-1D to 118-735B-11D indicate that we probably missed some of the deformational structures there.

Middle Structural Domain (Cores 118-735B-36R to 118-735B-56R; 172–272 mbsf)

The first interval of pervasive solid-state deformation is found in Cores 118-735B-37R to 118-735B-40R. Here, the finite strain is low (textural Types I and II), and the stretching lineation is dominantly downdip, but we found no reliable sense of shear criteria. The dynamically recrystallized plagioclase is polygonal and relatively large (about 20 to 30 μm). The other magmatic minerals have also recrystallized. The foliation underlined by these recrystallized minerals parallels the magmatic foliation in neighboring cores. This high T, probably low stress, and mostly anhydrous deformation may be a higher strain expression of the solid-state deformation overprint found in many magmatically foliated gabbros and inter-

preted as resulting from the last stages of flow in the progressively solidifying magma.

In Cores 118-735B-36R to 118-735B-51R, the magmatic foliation (with its downward decreasing dip; see "Magmatic Flow" section), and the high T, probably low-stress, solid-state foliation, are cut by millimeter- to meter-thick shear bands with a normal offset (Fig. 3). The foliation in these shear bands dips 15° to 50°, at a high angle to the magmatic and early solid-state structures, and often with a slightly different azimuth. The stretching lineation is downdip, and mylonitic textures are frequent. The dynamically recrystallized plagioclase is small (about 10 μm) and irregularly shaped. And the synkinematic assemblages are similar to those observed in the shear bands of the Upper Structural Domain: they indicate high T, low to moderate W/R ratio conditions in most samples, with locally continuing deformation at higher W/R ratio, lower T conditions (stability of actinolitic hornblende). The best developed example of these normal shear zones is the meter-thick mylonite of Core 118-735B-46R (Figs. 2 and 3). The mylonitic foliation there dips 15° to 30°, and the magmatic foliation above and below dips 20° to 40° in the opposite direction (Fig. 3).

In the deformed interval of Cores 118-735B-52R to 118-735B-56R, plastic deformation concentrated in two shear bands with textural Types II to V (Fig. 2). The foliation dips 0° to 25°, parallel to the flat-lying magmatic foliation in the overlying cores. The stretching lineation is downdip and the sense of shear, determined for four samples, is normal. The synkinematic assemblages indicate high T and low W/R ratio conditions (Fig. 2). The dynamically recrystallized plagioclase is polygonal and relatively large (about 15 to 30 μm ; Fig. 10), suggesting moderate deviatoric stresses. The geometrical relations of the shear bands of Cores 118-735B-52R to 118-735B-56R with the magmatic foliation, the moderate size of the plagioclase neoblasts, and the high T, low W/R ratio metamorphic assemblages, recall the characteristics of the solid-state deformation in Cores 118-735B-37R to 118-735B-40R. But the overall finite strain is larger (Fig. 2).

In Cores 118-735B-52R to 118-735B-54R, the foliation has been locally deformed by discontinuous millimeter-thick shear bands having the same azimuth, but a slightly steeper dip (mean dip: 25°) than the main foliation. These microscales have a normal offset and contain a large proportion of Fe-Ti oxides. Other normal shear bands are thicker (centimeter-thick) and steeper (25° to 40°), sometimes with a dip opposite that of the main foliation. The plagioclase, which recrystallized along these shear zones, is often irregular in shape and smaller (about 10 μm) than the plagioclase neoblasts found in the main foliation (Fig. 10).

Lastly, small volumes of late leucocratic melts intruded the gabbro in Cores 118-735B-49R to 118-735B-54R (Fig. 2). These late magmatic injections clearly disrupted the foliation of the deformed intervals. Most of these late magmatic intrusives are undeformed. But, in some samples, a slight deformation produced limited recrystallization of the late magmatic plagioclase in small (about 10 μm), irregularly shaped neoblasts (Fig. 4F).

The textures and metamorphic assemblages associated with the ductile deformation in the Middle Structural Domain, and the geometrical relations among the different families of structures, suggest a three-step tectonic evolution.

Step 1. Viscous laminar flow in the incompletely crystallized magma produced a magmatic foliation. This flow continued as the gabbro progressively solidified and produced a limited solid-state strain. The dip of the magmatic foliation (with its weak solid-state overprint) decreased downward, from 50–60° at 170 mbsf, to 0°–10° at 240 mbsf (Fig. 2). This

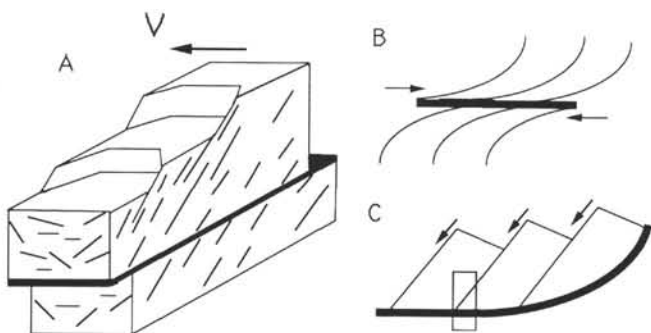


Figure 11. Upper Structural Domain. A. Schematic representation of the reorientation data presented by Cannat and Pariso (this volume); V = direction (declination) of the remanent magnetic vector; thin discontinuous lines = foliations above and below the horizontal mylonitic shear zone of Core 118-735B-6D (thick line). B. Sketch of a flat-lying shear zone (thick line), with progressive rotation of foliation (thin lines) above and below (see text). C. Sketch of a ductile listric normal fault (thick line), with set of associated planar ductile faults (thin lines); shaded area: possible location of the drill hole (see text).

progressive rotation probably occurred when the gabbro was not yet completely crystallized.

Step 2. The normal shear zones in the lower 30 m of the Middle Structural Domain developed at high T, probably moderate deviatoric stress, and mostly anhydrous conditions.

Step 3. Continuing solid-state deformation produced steeper millimeter- to meter-thick normal shear bands, at high to moderate T, often hydrous conditions. The late magmatic intrusives were injected in the gabbros toward the end of this deformation.

Lower Structural Domain (Cores 118-735B-56R to 118-735B-88N; 272–500.7 mbsf)

The olivine gabbros of Unit V and the upper 28 m of Unit VI are remarkably fresh and nearly undeformed (Fig. 2). In Cores 118-735B-58R to 118-735B-61R, a low-dipping magmatic foliation, parallel to a faint grain-size layering, is occasionally visible. Evidence for a limited high T, anhydrous solid-state flow causing recrystallization of plagioclase in relatively large polygonal neoblasts is found in two samples from Core 118-735B-73R (Fig. 10). This deformation did not produce a foliation in the rock. A weak deformation is also occasionally found in intervals of hydrothermally altered gabbros located near the late magmatic intrusives (Fig. 2). These altered gabbros are never foliated, but some samples are slightly deformed, with limited recrystallization of the plagioclase in small (about 5 to 10 μm), irregularly shaped neoblasts (Fig. 10). This limited plastic deformation occurred during the injection of the clinopyroxene-bearing hydrothermal veins (Stakes et al., this volume), as some of these veins are deformed, while others are undeformed and cut through the deformed zones.

Gabbros in the lower 97 m of the hole (Cores 118-735B-77R to 118-735B-88N; 403–500.7 mbsf) are moderately deformed. Centimeter- to meter-thick shear bands with textural Types I to III alternate with undeformed intervals (Fig. 2). Mylonitic intervals are thin (10 cm) and infrequent. The foliation in the shear bands dips 0° to 30° , and the stretching lineation is predominantly downdip. The synkinematic assemblages indicate high T, mostly anhydrous metamorphic conditions, but, in the lowermost cores (Cores 118-735B-85R to 118-735B-87R), synkinematic hornblende is locally abundant (Fig. 2).

In Cores 118-735B-76R to 118-735B-84R, the dynamically recrystallized plagioclase is relatively large (about 20 to 40 μm) and polygonal (Fig. 10). The sense of shear, determined in three samples, is normal. The foliation is locally cut and deformed by thin mylonitic shear zones, with a normal sense of shear (Fig. 9), and often steeper, sometimes conjugate, dips. These mylonites often developed in Fe-Ti oxide-rich zones and are typically associated with the recrystallization of small (about 10 μm), irregularly shaped plagioclase neoblasts. In Core 118-735B-78R, a small dikelet of late magmatic leucocratic melt crosscuts the moderately deformed gabbros, but was slightly sheared, with recrystallization of similar small plagioclase neoblasts. In Core 118-735B-77R, an early magmatic foliation, parallel to the solid-state foliation in this core, is locally preserved (Fig. 2). The tectonic evolution in Cores 118-735B-76R to 118-735B-84R therefore recalls the three-step scenario outlined for the Middle Structural Domain.

In Cores 118-735B-85R to 118-735B-87R, the recrystallization of plagioclase in small and irregularly shaped neoblasts is more pervasive than in the overlying cores. The sense of shear, determined in three samples, is still normal. The texture recalls that observed in the deformed gabbros of Unit II, in the Upper Structural Domain. Relicts of an earlier coarser-grained recrystallized texture are found in moderately strained intervals (Fig. 4E). A few synkinematic to late kinematic hornblende veins, perpendicular to the stretching

lineation in the gabbro, were observed in this interval (Fig. 12). But the amount of water that was present during deformation remained small, compared to what happened in the Upper Structural Domain, as there is never much hornblende recrystallized in the foliation (Fig. 2).

Meter-thick intervals of troctolites occur in Cores 118-735B-83R (459.7–461.8 mbsf), 118-735B-85R (478.4–479.7 mbsf), and 118-735B-87R (498.6–499.4 mbsf). The clear-cut contacts between these troctolites and the surrounding gabbros suggest intrusive, rather than cumulative, relations (Shipboard Scientific Party, 1989). These troctolites are composed of 30% to 40% olivine in lobate grains 1 mm to several millimeters in size, interdigitated with the plagioclase (Fig. 13). They occur in a well-deformed part of the hole, but exhibit little evidence of plastic deformation. The olivine displays subgrain boundaries, but is not recrystallized. The plagioclase is often mechanically twinned, but not recrystallized, except in one sample from Core 118-735B-83R having much less than 1% large (40–60 μm) polygonal plagioclase grains that may be neoblasts. During the early, high T, and probably moderate, stress deformation of the surrounding gabbros, ductile deformation mechanisms were active in both olivine and plagioclase (Cannat, this volume). This early event should therefore have deformed the troctolites; a possible explanation for why it did not is that the troctolites may have intruded the gabbros after the end of this moderate stress deformation. In contrast, during the latter, probably higher stress episode, olivine had a tendency to become brittle (Cannat, this volume). In the troctolites, the lobate olivine grains (Fig. 13) may then have behaved as a rigid frame, preventing plastic flow in the interdigitated plagioclase.

BRITTLE DEFORMATION IN THE SITE 735 GABBROS

The deformation accommodated by brittle failure at Site 735 appears minor, compared with the large strain accommo-



Figure 12. Hornblende veins sub-perpendicular to the downdip stretching lineation in Sample 118-735B-85R-4, 18–27 cm.

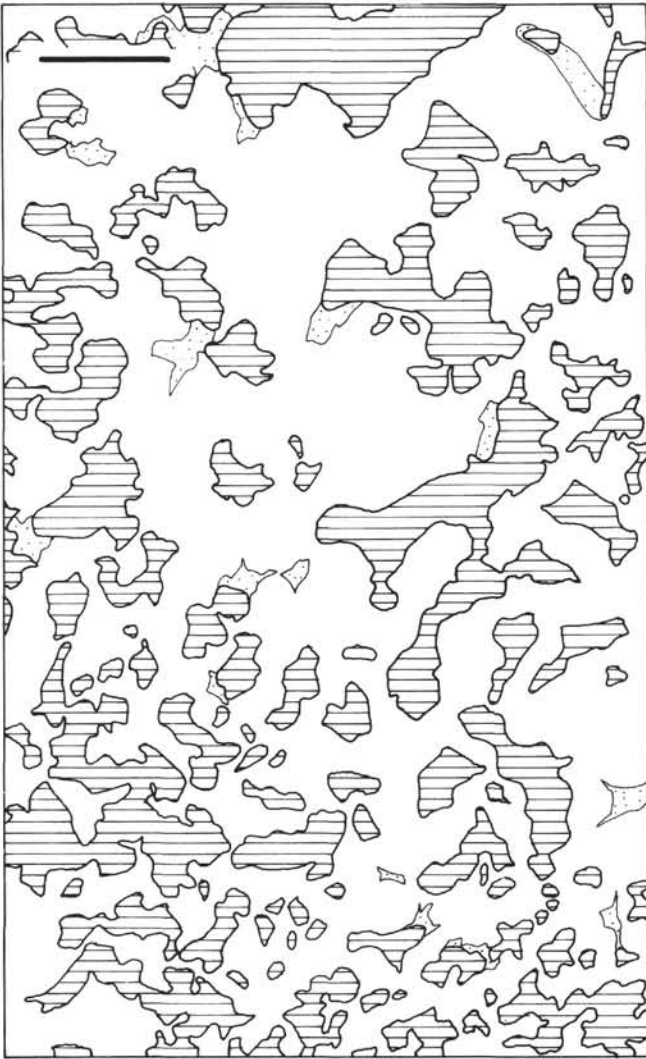


Figure 13. Troctolite Sample 118-735B-85R-6, 1020-111 cm. Scale bar = 0.5 cm. Horizontal lines = olivine; dots = clinopyroxene; white = plagioclase. The modal content of olivine, determined using image processing software "Visilog" (NOESIS, 1988), is 34%.

dated in the plastically deformed intervals. The features resulting from brittle deformation are millimeter- to centimeter-thick veins filled with a variety of hydrothermal minerals (hornblende, plagioclase, clinopyroxene, epidote, sphene, actinolite, chlorite, analcite, thomsonite, and calcite; Stakes et al., this volume). Centimeter- to decimeter-thick cataclastic intervals also developed locally, producing breccias with angular clasts of altered gabbro, separated by fractures filled with hydrothermal minerals (Fig. 4G). Shear displacements occurred along some of these fractures, but most hydrothermal minerals are undeformed, suggesting that the breccias were not subjected to much crushing after they were sealed. An origin by hydraulic fracturing during the injection of the hydrothermal fluids has been tentatively proposed for these breccias, which are frequent near the intrusions of late magmatic leucocratic melts.

The hornblende veins are filled with green to brown hornblende compositionally similar to the hornblende that crystallized in the foliation of plastically deformed gabbros (Stakes et al., this volume). These veins are most common in the upper part of the hole, and they are steeply dipping and often

subperpendicular to the stretching lineation developed in the surrounding gabbros during ductile deformation (Fig. 12). In thin section, crosscutting hornblende veins can be seen to have developed before the end of the ductile deformation, filling fractures in relict prophyroclasts boudinaged in the still plastically flowing recrystallized matrix (Fig. 4H). We propose that thick intervals of gabbros may have become boudinaged in a similar way between discrete mylonitic shear bands, producing the macroscopic hornblende veins subperpendicular to the stretching lineation (Fig. 12). In the uppermost part of the hole, the density of these synkinematic to late kinematic hornblende veins increases toward the mylonitic shear zone of Cores 118-735B-5D and 118-735B-6D (Fig. 7). The high chlorine content of the hornblende in these veins is similar to that of hornblende recrystallized in the mylonitic foliation (Stakes et al., this volume). This suggests that the mylonitic shear zone at Cores 118-735B-5D and 118-735B-6D acted as a pathway for high temperature, possibly seawater-derived, hydrous fluids. Some hornblende veins throughout the hole have been sheared, as indicated by the development of a foliation and lineation marked by the elongation of hornblende crystals. The lineation in most of these sheared veins is downdip, and the displacement had a dominant normal component (indicated by asymmetric tails around rotated hornblende prophyroclasts).

The veins filled with other hydrothermal minerals (plagioclase, clinopyroxene, epidote, sphene, actinolite, chlorite, analcite, thomsonite, and calcite) are often steeply dipping and also tend to be perpendicular to the foliation of the plastically deformed gabbros, but in contrast with hornblende, these other hydrothermal minerals do not fill synkinematic cracks in the plastically deformed gabbros. The clinopyroxene-bearing veins, common below 180 mbsf, may have been slightly deformed plastically, but always crosscut the foliation of the gabbros, showing no evidence that they may be synkinematic with respect to the main plastic deformation. These clinopyroxene-bearing veins are spatially, and possibly genetically, related to injections of late magmatic intrusives (Stakes et al., this volume). Those veins filled with lower temperature minerals, such as analcite, thomsonite or calcite, are never deformed.

INTERPRETATION

The tectonic evolution at Site 735 may be interpreted using the three-step scenario outlined for the Middle Structural Domain. These three steps are distinguished on the basis of apparent changes in the rheological behavior of the progressively cooling gabbros. The transition between Steps 2 and 3 is thought to have occurred in a context of progressive deformation. We will argue that this may also be the case for the transition between Steps 1 and 2.

Step 1. Viscous flow of the incompletely solidified magma produced a magmatic foliation, well-developed in the oxide-bearing gabbros of lithologic Units III and IV (Fig. 2). This flow took place in a crystal-mush that may represent the ridge axis magma chamber (Fig. 14). Recent seismic-reflection data about the fast-spreading East Pacific Rise suggest that the magma chamber *sensu stricto* is a thin region of high partial-melt fraction, surrounded by a much larger region of hot rocks, with isolated pockets of melt (Detrick et al., 1987; Harding et al., 1989). In the slow-spreading Southwest Indian Ridge context, where magma supply is likely to be small and perhaps discontinuous, this crystal-mush region may be even thinner and present only during transient melt emplacement events. Gravitational instabilities (convection) may induce viscous flow in this crystal-mush and produce the observed magmatic foliation. But this would not account for the parallel

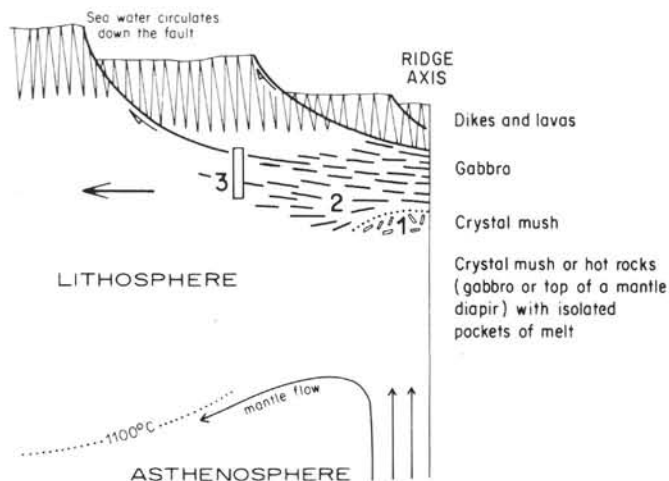


Figure 14. Interpretative sketch of tectonic evolution of Site 735 gabbros in the Southwest Indian Ridge axial region. Steps 1, 2, and 3 are discussed in text. Outline of drilled section gives an approximate scale (500 m). Lithosphere/asthenosphere boundary is drawn as the 1100°C isotherm (basalt solidus).

trend of this magmatic foliation and of the earliest solid-state deformation zones in many intervals throughout the hole. This parallel trend was directly observed in the core; it is also suggested by the reorientation data presented by Cannat and Pariso (this volume). To account for this observation, we propose that the progressively crystallizing magma was perhaps channeled along shear zones developing in already solidified gabbros above, or below the crystal-mush domain. Experimental data (Van der Molen and Paterson, 1979) suggest that the critical melt fraction separating magmatic flow behavior from solid-state flow is about 30 vol%. Progressive cooling and crystallization of a transient melt pocket in an environment subjected to tectonic stresses may produce the proposed coexistence of sheared intervals (less than 30% magma) with crystal-mush (more than 30% magma).

Step 2 corresponds to the early stages of solid-state ductile deformation in the gabbros (melt fraction: 0% to 30%; granulite-facies metamorphic conditions). We propose that it took place in, and in the immediate vicinity of, the transient crystal-mush region (Fig. 14). The relatively large size of the dynamically recrystallized plagioclase is thought to result from moderate deviatoric stresses, indicative of the low yield strength of the gabbros at that stage. The microstructural data presented by Cannat (this volume) suggest that during Step 2 strain localization leading to the formation of mylonites could only occur in intervals having more than 10% oxides. The oxide-poor gabbros thus probably behaved as a relatively continuous ductile unit during Step 2. Most of the ductile deformation in the lower part of the hole (Middle and Lower Structural Domains) occurred during Step 2, along low-dipping foliations (average 20°; Fig. 2). The sense of shear determinations are consistent with stretching of the newly crystallized crustal material (Fig. 14). The reorientation data presented by Cannat and Pariso (this volume) suggest that most foliations dipped roughly in the same direction. It also suggests that, at some point during Step 2, there was a shift (estimated at 45°; Cannat and Pariso, this volume) in the orientation of the principal strain directions: some foliations in the highly deformed intervals of Cores 118-735B-52R to 118-735B-56R, and of Cores 118-735B-77R to 118-735B-88N (Fig. 2), appear oblique with respect to the Step 2 foliation in other intervals, which parallels the magmatic foliation.

Step 3 corresponds to the continuation of the ductile deformation in the gabbros, at progressively decreasing temperatures (upper amphibolite- to actinolite-facies metamorphic conditions), and with increased availability of water. The small size of the dynamically recrystallized plagioclase is thought to result from relatively high deviatoric stresses, reflecting an increase in the yield strength of the gabbros between Steps 2 and 3. The deformation during Step 3 became strongly localized in mylonitic shear bands, which may have been pathways for the circulation of water-rich hydrothermal fluids. Strain localization in mylonitic bands was probably accompanied by brittle failure and boudinage in the less deformed intervals. Most deformation in the Upper Structural Domain occurred during Step 3. Foliation dips there varied between 0° and 70° (Fig. 2): 0° in the main mylonitic shear zones and an average of 35° in the less deformed intervals. Most sense of shear determinations are consistent with normal shearing and suggest that stretching of the crust continued during Step 3. The reorientation data presented by Cannat and Pariso (this volume) suggest that the foliations produced during Step 3 dipped approximately in the same direction than the late Step 2 foliations (i.e., at an angle to the magmatic and early Step 2 foliations). Step 3 represents the last stages of ductile deformation recorded at Site 735. In Figure 14, we propose that Step 3 occurred as the progressively cooled gabbros moved away from the ridge axis. It may also have occurred at the ridge axis itself, during a period when the magma supply was too small to compensate the conductive and hydrothermal cooling processes.

The present-day setting of the crust at Site 735 suggests that it has been accreted at the ridge, some 18 km to the east of the Southwest Indian Ridge/Atlantis II Fracture Zone intersection (Fig. 1). It is likely that a large offset fracture zone, such as Atlantis II, has a deep influence on the asthenospheric flow below adjacent ridge segments (Fox and Gallo, 1984; Morgan and Forsyth, 1988). The tectonic evolution of the Site 735 gabbros may thus be related to ridge/transform intersection processes. But this is also likely to be the case along much of the Southwest Indian Ridge, because 18 km actually represents about one-half the average length of the ridge segments in this part of the Indian Ocean (Fisher and Sclater, 1983). Large-scale, moderately dipping, normal faults in the newly created lithosphere of ridge/transform intersection domains have been documented in the Atlantic Ocean by a seismic survey in the Vema Fracture Zone (Bowen and White, 1986) and by submersible observations in the Kane Fracture Zone area (Dick et al., 1981; Karson and Dick, 1984; Mével et al., 1988; Mével et al., in press). In Figure 14, we postulate that the low-dipping extensional ductile shear zones at Site 735 (Fig. 14) represent the deep-seated expression of such normal faults. We therefore have drawn these faults with a listric geometry, which recalls the hypothesis postulated in Figure 11C for the mylonitic shear zone of Cores 118-735B-5D and 118-735B-6D. Note that listric faulting (as drawn in Fig. 14) does not necessarily imply significant tilting of the faulted blocks, because intense ductile deformation may have taken place at depth, along the edges of these blocks. Note also that the volcanic carapace sketched in Figure 14 is relatively thin (the outline of the Site 735, 500-m-deep drill hole may be used as an approximate scale). This is based on the hypothesis that the magmatic budget at the Southwest Indian Ridge was low during the accretion of the Site 735 gabbros.

Finally, we end this interpretation on a note of caution: an important assumption made in Figure 14 is that the ductile shear zones sampled at Site 735 dipped toward the Southwest Indian Ridge axis, or at a moderate angle to it. At this point, we have no information about the azimuth of these structures.

They have been partially reoriented relative to the *in-situ* remanent magnetic vector (Cannat and Pariso, this volume), but the azimuth of this vector is unknown. The geometry of the shear zones (as drawn in Fig. 14) therefore is hypothetical.

ACKNOWLEDGMENTS

This work was financially supported by ODP-FRANCE (ATP-ODP to M.C. and C.M.) and by NSF and JOI-USSAC grants (OCE-8902586 and Texas A&M FD20195 to D.S.). We thank our reviewers for their helpful advice, and J-L. Travers (UBO, Brest) for his help with the graphics.

REFERENCES

- Benn, K., and Allard, B., 1989. Preferred mineral orientations related to magmatic flow in ophiolite layered gabbros. *J. Petrol.*, 30:925–946.
- Bird, J. E., Mukherjee, A. K., and Dorn, J. F., 1969. Correlations between high temperature creep behaviour and structure. In Brandon, D. G., and Rosen, R. (Eds), *Quantitative Relation Between Properties and Microstructure*: Haifa, Israel, 255–342.
- Bonatti, E., Honnorez, J., Kirst, P., and Radicatti, F., 1975. Metagabbros from the Mid-Atlantic Ridge at 06°N: contact hydrothermal dynamic metamorphism beneath the axial valley. *J. Geol.*, 83:61–78.
- Bonatti, E., and Honnorez, J., 1976. Sections of the earth's crust in the Equatorial Atlantic. *J. Geophys. Res.*, 81:4104–4116.
- Bowen, A. N., and White, R. S., 1986. Deep-tow seismic profiles from the Vema Transform and Ridge/Transform intersection. *J. Geol. Soc. London*, 143:807–817.
- Cannat, M., Juteau, T., and Berger, E., 1990. Petrostructural analysis of the Leg 109 serpentinitized peridotites. In Detrick, R., Honnorez, J., Bryan, W. B., Juteau, T., et al., *Proc. ODP, Sci. Results*, Vol. 106/109: College Station, TX (Ocean Drilling Program), 47–56.
- CAYTROUGH, 1979. Geological and geophysical investigation of the Mid-Cayman Rise spreading center: initial results and observations. In Talwani, M., Harrison, C. G., and Hayes, D. E. (Eds), *Deep Drilling Results in the Atlantic Ocean: Ocean Crust*. Maurice Ewing Ser., Vol. 2, 66–93.
- Detrick, R. S., Buhl, P., Vera, E. E., Mutter, J., Orcutt, J. A., Madsen, J., and Brocher, T., 1987. Multichannel seismic imaging of an axial magma chamber along the East Pacific Rise between 9°N and 13°N. *Nature*, 326:35–41.
- Dick, H.J.B., Thompson, G., and Bryan, W. B., 1981. Low angle faulting and steady-state emplacement of plutonic rocks at ridge/transform intersections. *EOS (Abs.)*, 62:406.
- Fisher, R. L., and Sclater, J. G., 1983. Tectonic evolution of the Southwest Indian Ocean since Mid-Cretaceous: plate motions and stability of the pole of Antarctica/Africa for at least 80 Myr. *Geophys. J. Royal Astron. Soc.*, 73:553–576.
- Fisher, R. L., Dick, H.J.B., Natland, J. H., and Meyer, P. S., 1986. Mafic/ultramafic suites of the slowly spreading Southwest Indian Ridge: Protea exploration of the Antarctic plate boundary, 24°E–47°E, 1984. *Ophioliti*, 11:147–178.
- Fox, P. J., Detrick, R., and Purdy, G. M., 1980. Evidence for crustal thinning near fracture zones: implications for ophiolites. In Panayiotou, A. (Ed.), *Ophiolites: Proc. Int. Ophiolite Symp.*: Cyprus, Geol. Surv. Dept., 161–168.
- Fox, P. J., and Gallo, D., 1984. A tectonic model for ridge-transform-ridge plate boundaries: implications for the structure of oceanic lithosphere. *Tectonophysics*, 104:205–242.
- Francis, T. G., 1981. Serpentinization faults and their role in the tectonics of slow spreading ridges. *J. Geophys. Res.*, 86:11616–11622.
- Harding, A. J., Orcutt, J. A., Kappus, M. E., Vera, E. E., Mutter, J. C., Buhl, P., Detrick, R. S., and Brocher, T. M., 1989. The structure of young oceanic crust at 13°N on the East Pacific Rise from expanding spread profiles. *J. Geophys. Res.*, 94:12163–12196.
- Helmstaedt, H., and Allen, J. M., 1977. Metagabbroites from DSDP hole 334. An example of high temperature deformation and recrystallization near the Mid-Atlantic Ridge. *Can. J. Sci.*, 14:886–898.
- Honnorez, J., Mével, C., and Montigny, R., 1984. Geotectonic significance of gneissic amphibolites from the Vema fracture zone, Equatorial Mid-Atlantic Ridge. *J. Geophys. Res.*, 89:11379–11400.
- Ito, E., and Anderson, A. T., 1983. Submarine metamorphism of gabbro from the Mid-Cayman Rise: petrographic and mineralogical constraints on hydrothermal processes at slow spreading ridges. *Contrib. Mineral. Petrol.*, 82:371–388.
- Karson, J. A., in press. Seafloor spreading on the Mid-Atlantic Ridge: implications for the structure of ophiolites and oceanic lithosphere produced in slow-spreading environments. *Proc. Symp. Ophiolites Oceanic Lithos.* (Troodos, 1987).
- Karson, J. A., and Dick, H.J.B., 1984. Deformed and metamorphosed oceanic crust on the Mid-Atlantic Ridge. *Ophioliti*, 9:279–302.
- Mercier, J.-C., Anderson, D. A., and Carter, N. L., 1977. Stress in the lithosphere: inferences from steady-state flow of rocks. *Pure Appl. Geophys.*, 115:199–226.
- Mével, C., 1987. Evolution of oceanic gabbros from DSDP Leg 82: influence of the fluid phase on metamorphic crystallizations. *Earth Planet. Sci. Lett.*, 83:67–79.
- , 1988. Metamorphism in oceanic layer 3, Goringe Bank, eastern Atlantic. *Contrib. Mineral. Petrol.*, 100:496–509.
- Mével, C., Auzende, J.-M., Cannat, M., Donval, J.-P., Dubois, J., Fouquet, Y., Gente, P., Grimaud, D., Karson, J. A., Segonzac, M., and Stievenard, M., 1988. Hydrosnake 1988: submersible study of seafloor spreading in the MARK area. *EOS (Abs.)*, 69:1439–1440.
- Mével, C., Cannat, M., Gente, P., Marion, E., Auzende, J.-M., and Karson, J. A., in press. Emplacement of deep rocks on the west median valley wall of the MARK area (M.A.R., 23°N). *Tectonophysics*.
- Morgan, J. P., and Forsyth, D. W., 1988. Three-dimensional flow and temperature perturbations due to a transform offset: effects on oceanic crustal and upper mantle structure. *J. Geophys. Res.*, 93:2955–2966.
- NOESIS, 1988. "Visilog," a Computer Vision Software: Versailles, France.
- Shipboard Scientific Party, 1989. Site 735. In Robinson, P. T., and Von Herzen, R., et al., *Proc. ODP, Init. Repts.*, 118: College Station, TX (Ocean Drilling Program), 89–212.
- Stakes, D. S., and Vanko, D. A., 1986. Multistage alteration of gabbroic rocks from the failed Mathematician Ridge. *Earth Planet. Sci. Lett.*, 79:75–92.
- Twiss, R. J., 1977. Theory and applicability of a recrystallized grain size paleopiezometer. *Pure Appl. Geophys.*, 115:227–244.
- Van der Molen, I., and Paterson, M. S., 1979. Experimental deformation of partially melted granite. *Contrib. Mineral. Petrol.*, 70:299–318.
- Wernicke, B., and Burchfiel, B. C., 1982. Modes of extensional tectonics. *J. Struct. Geol.*, 4:105–115.

Date of initial receipt: 11 July 1989

Date of acceptance: 5 April 1990

Ms 118B-157